



Prolonged culture of human pancreatic islets under glucotoxic conditions changes their acute beta cell calcium and insulin secretion glucose response curves from sigmoid to bell-shaped

Mohammad Tariq^{1,2} · Arnaldo H. de Souza¹ · Mohammed Bensellam¹ · Heeyoung Chae¹ · Manon Jaffredo³ · Anne-Françoise Close¹ · Jean-Philippe Deglasse¹ · Laila R. B. Santos^{1,4} · Antoine Buemi⁵ · Nizar I. Mourad⁵ · Anne Wojtusciszyn^{6,7} · Matthieu Raoux³ · Patrick Gilon¹ · Christophe Broca⁶ · Jean-Christophe Jonas¹

Received: 9 June 2022 / Accepted: 18 October 2022 / Published online: 2 December 2022
© The Author(s), under exclusive licence to Springer-Verlag GmbH Germany, part of Springer Nature 2022

Abstract

Aims/hypothesis The rapid remission of type 2 diabetes by a diet very low in energy correlates with a marked improvement in glucose-stimulated insulin secretion (GSIS), emphasising the role of beta cell dysfunction in the early stages of the disease. In search of novel mechanisms of beta cell dysfunction after long-term exposure to mild to severe glucotoxic conditions, we extensively characterised the alterations in insulin secretion and upstream coupling events in human islets cultured for 1–3 weeks at ~5, 8, 10 or 20 mmol/l glucose and subsequently stimulated by an acute stepwise increase in glucose concentration.

Methods Human islets from 49 non-diabetic donors (ND-islets) and six type 2 diabetic donors (T2D-islets) were obtained from five isolation centres. After shipment, the islets were precultured for 3–7 days in RPMI medium containing ~5 mmol/l glucose and 10% (vol/vol) heat-inactivated FBS with selective islet picking at each medium renewal. Islets were then cultured for 1–3 weeks in RPMI containing ~5, 8, 10 or 20 mmol/l glucose before measurement of insulin secretion during culture, islet insulin and DNA content, beta cell apoptosis and cytosolic and mitochondrial glutathione redox state, and assessment of dynamic insulin secretion and upstream coupling events during acute stepwise stimulation with glucose [NAD(P)H autofluorescence, ATP/(ATP+ADP) ratio, electrical activity, cytosolic Ca²⁺ concentration ([Ca²⁺]_c)].

Results Culture of ND-islets for 1–3 weeks at 8, 10 or 20 vs 5 mmol/l glucose did not significantly increase beta cell apoptosis or oxidative stress but decreased insulin content in a concentration-dependent manner and increased beta cell sensitivity to subsequent acute stimulation with glucose. Islet glucose responsiveness was higher after culture at 8 or 10 vs 5 mmol/l glucose and markedly reduced after culture at 20 vs 5 mmol/l glucose. In addition, the [Ca²⁺]_c and insulin secretion responses to acute stepwise stimulation with glucose were no longer sigmoid but bell-shaped, with maximal stimulation at 5 or 10 mmol/l glucose and rapid sustained inhibition above that concentration. Such paradoxical inhibition was, however, no longer observed when islets were acutely depolarised by 30 mmol/l extracellular K⁺. The glucotoxic alterations of beta cell function were fully

Anne-Françoise Close and Jean-Philippe Deglasse contributed significantly to the study over the last 10 years but are no longer affiliated with a research laboratory. They are listed in alphabetical order.

✉ Jean-Christophe Jonas
jean-christophe.jonas@uclouvain.be

¹ Secteur des sciences de la santé, Institut de recherche expérimentale et clinique, Pôle d'endocrinologie, diabète et nutrition, Université catholique de Louvain, Brussels, Belgium

² Present address: Lund University Diabetes Centre, Department of Clinical Sciences, Lund University, Malmö, Sweden

³ CNRS, Institute of Chemistry and Biology of Membranes and Nano-objects, UMR 5248, University of Bordeaux, Pessac, France

⁴ Present address: Bio Base Europe Pilot Plant (BBEPP), Ghent, Belgium

⁵ Secteur des sciences de la santé, Institut de recherche expérimentale et clinique, Pôle de chirurgie expérimentale, Université catholique de Louvain, Brussels, Belgium

⁶ Laboratoire de Thérapie Cellulaire du Diabète, Institut de Médecine Régénérative et Biothérapies, Hôpital St Eloi, CHU Montpellier, Montpellier, France

⁷ Present address: Service d'Endocrinologie, Diabétologie et Métabolisme, Centre Hospitalier Universitaire Vaudois and Université de Lausanne, Lausanne, Switzerland

Research in context

What is already known about this subject?

- Culture of rodent islets at high glucose concentrations alters beta cell function and survival
- Culture of human islets at high glucose concentrations alters beta cell function with little increase in apoptosis
- Culture of rodent and human islets at high glucose concentrations increases beta cell glucose sensitivity and lowers beta cell glucose responsiveness

What is the key question?

- What are the alterations in beta cell responses to acute stepwise stimulation with glucose (insulin secretion and upstream coupling events) in non-diabetic and type 2 diabetic human islets cultured for 1–3 weeks at intermediate and high vs normal glucose concentrations?

What are the new findings?

- After 1–3 weeks of culture at 8–20 mmol/l glucose, human islets display a paradoxical inhibition of Ca^{2+} and insulin secretion on acute stimulation above 5 or 10 mmol/l glucose
- This acute inhibition is not associated with a decrease in glucose metabolism but is likely to result from acute plasma membrane repolarisation
- In human islets cultured under glucotoxic conditions, the acute Ca^{2+} and insulin secretion glucose response curves are bell-shaped

How might this impact on clinical practice in the foreseeable future?

- If this paradoxical glucose response is operational in vivo, characterising its mechanism may help identify new ways to improve beta cell function and reverse recently diagnosed type 2 diabetes

reversible after culture at 5 mmol/l glucose and were mimicked by pharmacological activation of glucokinase during culture at 5 mmol/l glucose. Similar results to those seen in ND-islets were obtained in T2D-islets, except that their rate of insulin secretion during culture at 8 and 20 mmol/l glucose was lower, their cytosolic glutathione oxidation increased after culture at 8 and 20 mmol/l glucose, and the alterations in GSIS and upstream coupling events were greater after culture at 8 mmol/l glucose.

Conclusions/interpretation Prolonged culture of human islets under moderate to severe glucotoxic conditions markedly increased their glucose sensitivity and revealed a bell-shaped acute glucose response curve for changes in $[\text{Ca}^{2+}]_c$ and insulin secretion, with maximal stimulation at 5 or 10 mmol/l glucose and rapid inhibition above that concentration. This novel glucotoxic alteration may contribute to beta cell dysfunction in type 2 diabetes independently from a detectable increase in beta cell apoptosis.

Keywords Cytosolic calcium · Glucose response curve · Glucotoxicity · Human islets · Long-term culture

Abbreviations

$[\text{Ca}^{2+}]_c$	Cytosolic Ca^{2+} concentration
E_{GSH}	Glutathione redox state
GSIS	Glucose-stimulated insulin secretion
K30Dz	30 mmol/l extracellular K^+ in the presence of diazoxide
ND-islets	Non-diabetic islets
SP	Slow potential
T2D-islets	Type 2 diabetic islets

Introduction

Pancreatic beta cells are critical for glucose homeostasis owing to their ability to constantly adapt insulin secretion to changes in the concentrations of glucose and other nutrients. In humans and rodents, glucose-stimulated insulin secretion (GSIS) results from an acceleration of glucose metabolism with a rise in the NAD(P)H/NAD(P)^+ and ATP/ADP ratios, closure of ATP-sensitive K^+ channels,

plasma membrane depolarisation, opening of voltage-dependent Ca^{2+} channels and Ca^{2+} influx, with the rise in cytosolic Ca^{2+} concentration ($[\text{Ca}^{2+}]_c$) triggering insulin granule exocytosis [1–3]. In addition, glucose metabolism amplifies Ca^{2+} -induced exocytosis [4]. In the context of glucose intolerance and type 2 diabetes, chronic exposure to the diabetic milieu slowly alters beta cell mass and function, thereby aggravating the disease [5, 6]. Although the relative contributions of glucose and lipids to nutrient toxicity are debated, several studies in rodents have demonstrated a major contribution of glucotoxicity to the reversible alterations of beta cell gene expression, loss of insulin content and GSIS, and apoptosis in diabetes, and a beneficial impact of beta cell rest on some of these alterations [7–13]. In comparison, human beta cells in culture or humanised murine models of diabetes are less prone to glucotoxic apoptosis unless concomitantly exposed to high levels of saturated NEFAs [12, 14, 15]. Moreover, a decrease in beta cell function rather than number probably contributes to the alterations in GSIS in early type 2 diabetes. Indeed, in obese patients with recent type 2 diabetes submitted to severe energy restriction, the remission of diabetes critically depends on rapid restoration of beta cell glucose responsiveness [16, 17]. Here, we tested the impact of 1–3 weeks of culture at various glucose concentrations on human islets from non-diabetic and type 2 diabetic donors. As beta cell apoptosis did not increase, we thoroughly analysed insulin secretion and upstream coupling events during stepwise stimulation with glucose, looking for yet unrecognised glucotoxic alterations in human beta cell stimulus–secretion events.

Methods

For detailed methods, please see the [electronic supplementary material](#) (ESM).

Islet preparations Islets were isolated with informed consent from 49 non-diabetic donors (ND-islets) and six donors with a history of type 2 diabetes (T2D-islets) in five isolation centres. Islets were cultured and shipped in CMRL medium containing 5.5 mmol/l glucose and 10% (vol/vol) FBS or 59 g/l human serum albumin. Donor and islet preparation characteristics are shown in Table 1 and ESM Table 1. Experiments were approved by the UCL-Saint-Luc ethics committee (project 2017/05JUL/355).

Islet culture Islets were precultured for 4–7 days in RPMI medium containing 5.5 mmol/l glucose and 10% (vol/vol) FBS or 5 g/l BSA, with hand-picking to another dish every 2–3 days and removal of islets with detectable central necrosis at $\times 10$ magnification. Islets were then cultured for 1–3 weeks in RPMI medium containing ~5.5, 8.5, 10.5 or 20.5 mmol/l glucose (referred to as G5-, G8-, G10- and G20-islets throughout the paper). Insulin was measured in the culture medium (renewed every 2–3 days) using an in-house RIA with human insulin as a standard.

Apoptosis and proportion of alpha and beta cells Islet histone-associated DNA fragments were quantified using a commercial ELISA. The results were normalised to DNA content measured by fluorimetry. The percentage of beta cell

Table 1 Summary of the characteristics of donors and islet preparations

Descriptive statistics	Age	Sex ratio (M/F)	BMI (kg/m^2)	HbA _{1c} (%)	HbA _{1c} (mmol/mol)	Cold ischaemia duration (h)	Islet purity (%)	Culture time until reception (h)
Donors with no history of diabetes								
<i>n</i>	49	31/18	49	12	12	41	46	49
Min.	17		20.5	4.5	25.5	2	75	6
Max.	74		40.2	6.1	43.1	23	95	170
Median	55		25.7	5.5	36.5	8	90	96
Mean	54		26.6	5.4	35.4	9	87	95
Donors with a history of type 2 diabetes								
<i>n</i>	6	6/0	6	2	2	6	6	6
Min.	43		25.4	6.0	42	4	80	60
Max.	68		30.5	6.5	47.5	11	90	168
Median	61		27.9	6.3	45.3	8	83	125
Mean	59		27.9	6.3	45.3	8	84	116

Details for each donor and islet preparation can be found in ESM Table 1. The numbers of donors/preparations for which the data were available are shown on the first line of each column

apoptosis was determined by TUNEL assay and insulin immunodetection in islet sections (ESM Fig. 1). Central necrotic areas were excluded from counting. Other islet sections were used to compute the proportion of alpha and beta cells after immunodetection of glucagon- and insulin-positive cells.

Glutathione redox state Cytosolic and mitochondrial glutathione redox state (E_{GSH}) were measured as indicators of cytosolic and mitochondrial oxidative stress in islets expressing roGFP1 or mt-roGFP1. The probe fluorescence ratio was normalised to the minimal ratio (set to 0%) in dithiothreitol and the maximum ratio (set to 100%) in aldrithiol [18, 19].

Solutions Acute glucose responses were measured using KRB containing (in mmol/l) NaCl (124), KCl (4.8), CaCl_2 (2.5), MgCl_2 (1.2) and NaHCO_3 (20), 1 g/l BSA (fraction V; Roche) and n mmol/l glucose (G_n). When KCl was raised to 30 mmol/l, NaCl was reduced to 98.8 mmol/l. The solutions were continuously gassed with 5% (vol/vol) CO_2 in pure O_2 to maintain a pH of ~ 7.4 at 37°C .

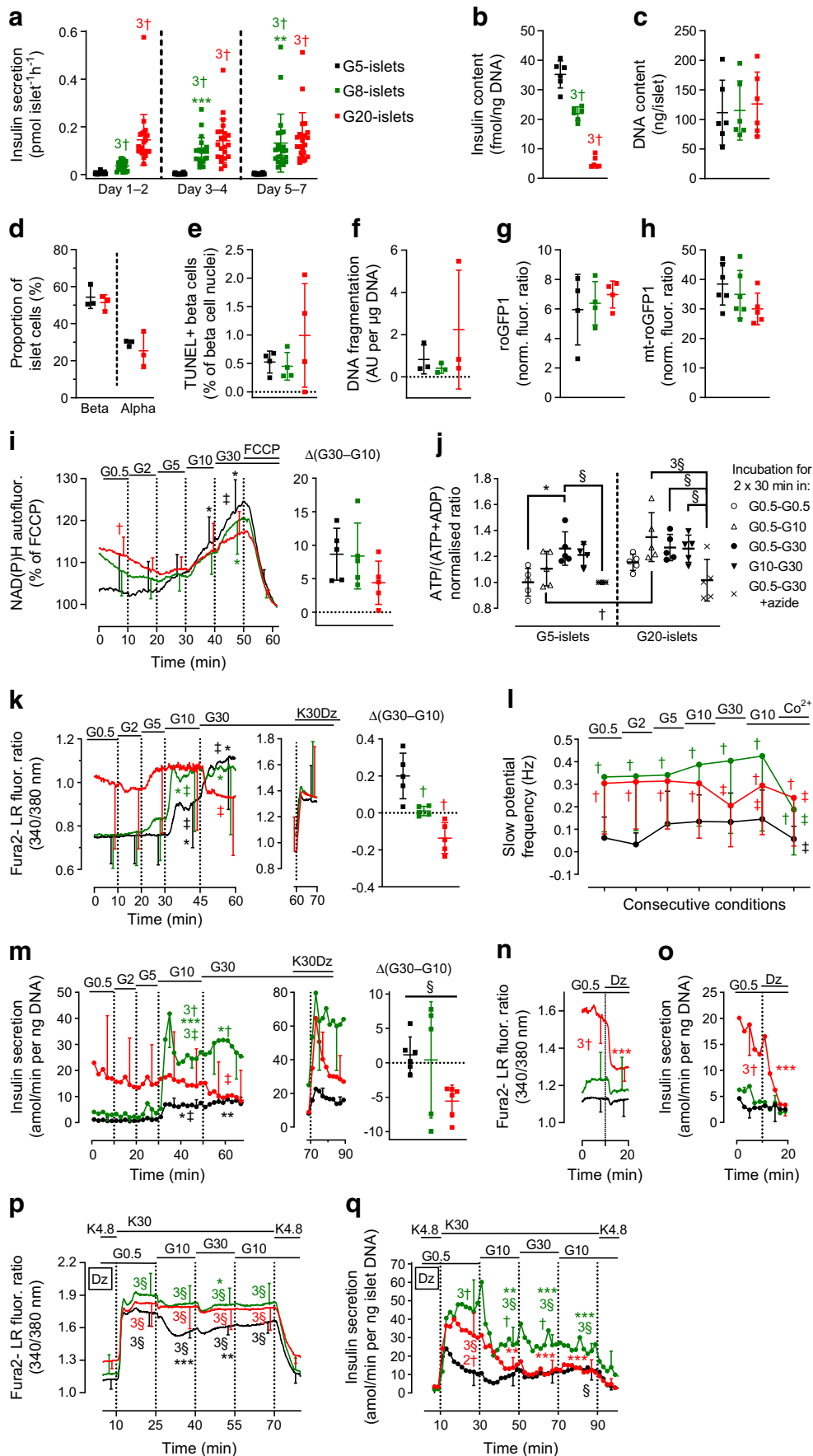
ATP measurements After 30 min preincubation in KRB containing 0.5 mmol/l glucose, islets were incubated for 30 min in 0.5 or 10 mmol/l glucose before incubating for 30 min at various glucose concentrations. ATP and ATP+ADP were measured using a luminometric method [20]; the ATP/(ATP+ADP) ratio was computed and normalised to the ratio in G5-islets treated with azide.

NAD(P)H, $[\text{Ca}^{2+}]_c$ and insulin secretion After 30 min perfusion with KRB containing 0.5 mmol/l glucose, islets were stimulated with increasing glucose concentrations. NAD(P)H autofluorescence and $[\text{Ca}^{2+}]_c$ were measured in small- to medium-sized islets (diameter ~ 75 – 150 μm) [21]. $[\text{Ca}^{2+}]_c$ was measured by recording the fura2-LR fluorescence ratio in islets loaded with 2 $\mu\text{mol/l}$ fura2-LR-acetoxymethylester at the same glucose concentration as during culture [21]. Alternatively, islets were infected with Ad-RIP-D3cpv and the probe fluorescence ratio was recorded. Insulin secretion was measured in 2 min effluent collections from 100–150 perfused islets (diameter ~ 75 – 330 μm). The islet DNA and insulin contents were measured after perfusion and used for data normalisation.

Electrical activity Islets were seeded on multielectrode arrays coated with Matrigel. After 1 week of culture at G5, G8 or G20, islets were perfused with HEPES-buffered KRB at various glucose concentrations with the final addition of 1 mmol/l

Fig. 1 Long-term (1 week) effects of glucose on cultured human islets. After preculture at G5, human islets were cultured for 1 week in RPMI medium containing G5, G8 or G20 (G5-islets, black; G8-islets, green; G20-islets, red). **(a)** Insulin secreted in the culture medium, which was collected every 2–3 days. Means \pm SD and individual data for the 22 preparations used for the experiments shown in Fig. 1. **(b)** Islet insulin/DNA content ratio and **(c)** DNA content at the end of the experiments shown in **(m)**. Means \pm SD and individual data for six preparations. **(d)** Proportions of beta and alpha cells and **(e)** percentage of TUNEL-positive beta cells in islet sections. Means \pm SD and individual data for three to four preparations. **(f)** Islet histone-associated cytosolic DNA fragments after culture (absorbance arbitrary units normalised for differences in islet DNA content). Means \pm SD and individual data for three preparations. **(g)** Cytosolic and **(h)** mitochondrial E_{GSH} as reflected by the roGFP1 and mt-roGFP1 normalised fluorescence ratio, respectively (see Methods). Means \pm SD and individual data for four **(g)** or six **(h)** preparations. **(i)** NAD(P)H autofluorescence during stimulation with a stepwise increase in glucose concentration (G_n , n mmol/l glucose), as indicated at the top of the figure. Data from each islet were normalised to the fluorescence level measured 10 min after the addition of 10 $\mu\text{mol/l}$ FCCP. Means \pm SD for five preparations, each with one or two islets. The $\Delta(\text{G30-G10})$ graph shows the change in NAD(P)H autofluorescence between the 10 and 30 mmol/l glucose steps calculated by subtracting the mean data over the last 3 min for G10 from the mean data over the last 3 min for G30; units are as in the graphs showing the corresponding dynamic traces. **(j)** ATP/(ATP+ADP) ratio in islets incubated for two consecutive periods of 30 min at the indicated glucose concentrations. In each experiment, the ratios were normalised to that measured in G5-islets incubated in 30 mmol/l glucose + 5 mmol/l azide. Means \pm SD and individual data for five preparations, each with two to three batches of 10 islets per condition. **(k)** Fura2-LR fluorescence ratio (as an indicator of $[\text{Ca}^{2+}]_c$) and **(m)** insulin secretion rate during stepwise glucose stimulation followed by membrane depolarisation with 30 mmol/l extracellular K^+ in the presence of 250 $\mu\text{mol/l}$ diazoxide (K30Dz). Means \pm SD for five to six preparations. The $\Delta(\text{G30-G10})$ graphs show the changes in fura2-LR fluorescence ratio and insulin secretion rate between the 10 and 30 mmol/l glucose steps calculated as in **(i)** using the mean data during the last 3 min **(k)** or 6 min **(m)** of each step. **(l)** Electrical activity recorded with MEAs in islets stimulated by a stepwise increase in glucose concentration, as indicated at the top of the figure. The mean SP frequencies were computed over the last 5 min of each condition. Co^{2+} , 1 mmol/l CoCl_2 . Data are means \pm SD for 14–27 measurements from three islet preparations. For more details, see ESM Fig. 4. **(n, o)** Effect of 100 $\mu\text{mol/l}$ diazoxide (Dz) on $[\text{Ca}^{2+}]_c$ **(n)** and insulin secretion **(o)** during perfusion at 0.5 mmol/l glucose. Means \pm SD for four or five preparations. **(p)** Fura2-LR fluorescence ratio and **(q)** insulin secretion rate during acute depolarisation with 30 mmol/l extracellular K^+ (K30) in the presence of 0.5 mmol/l glucose and 100 $\mu\text{mol/l}$ Dz followed by stepwise glucose stimulation. Means \pm SD for four to five preparations. Statistical analysis: (**[a, j]**) and dynamic recordings in **[i, k–q]**) Two-way ANOVA plus Tukey's test: * $p < 0.05$, ** $p < 0.01$ and *** $p < 0.001$ vs day 1–2 **(a)** or G0.5 step **(i–q)** in the same islet type; † $p < 0.05$, 2† $p < 0.01$ and 3† $p < 0.001$ vs G5-islets at the same time point; ‡ $p < 0.05$ and 3‡ $p < 0.001$ vs previous step in the same islet type; § $p < 0.05$ and 3§ $p < 0.001$ vs azide **(j)** or vs initial step before K30 stimulation **(p, q)**. (**[b–h]**) and Δ graphs in **[i, k, m]**) One-way ANOVA plus Dunnett's test: † $p < 0.05$, 2† $p < 0.01$ and 3† $p < 0.001$ vs G5-islets; test for linear trend from left to right: § $p < 0.05$

CoCl_2 . Extracellular field potentials were acquired and treated as described [22]. Slow potentials (SPs), which are multicellular beta cell-specific signals resulting from beta cell coupling [23], were isolated as described in Lebreton et al [23]. Mean SP frequencies were determined over the last 5 min of each condition for each recorded islet.



Statistics Means \pm SD are shown for the number of preparations/donors indicated, with individual data added to the column bars. The statistical significance of differences between groups was evaluated by one-way ANOVA followed by Dunnett's test or a test for linear trend, or by two-way ANOVA (for repeated measurements when comparing selected time points in the same trace) followed by Tukey's test, or by mixed-effects model analysis followed by Sidak's test when few data were missing. Analyses were carried out using GraphPad Prism version 9 (USA).

Results

Impact of culture for 1 week at increasing glucose concentrations on insulin secretion, islet insulin and DNA content, beta cell apoptosis, and cytosolic and mitochondrial glutathione redox state During culture, insulin secretion was significantly higher in G8-islets and G20-islets than in G5-islets, with a time-dependent increase in G8-islets (Fig. 1a). After culture, the insulin content was \sim 33% lower in G8-islets and \sim 85% lower in G20-islets than in G5-islets (Fig. 1b), while the DNA content was unaffected (Fig. 1c). The proportions of beta and alpha cells were also similar in G5-islets and G20-islets (Fig. 1d). DNA fragmentation, percentage of TUNEL-positive beta cells, cytosolic E_{GSH} (a marker of cytosolic oxidative stress) and mitochondrial E_{GSH} did not differ significantly between groups (Fig. 1e–h). We obtained similar results after culture in FBS-free medium containing BSA (ESM Fig. 2).

Impact of culture for 1 week at increasing glucose concentrations on subsequent GISIS and upstream coupling events After culture, the responses to stepwise increases in glucose concentration were measured after a \sim 30 min exposure to 0.5 mmol/l glucose (Fig. 1 and ESM Fig. 3). To compare glucose metabolism between groups, NAD(P)H autofluorescence and the ATP/(ATP+ADP) ratio were normalised to their minimums in the presence of the mitochondrial poisons FCCP (uncoupler) or azide (complex IV inhibitor).

In G5-islets, glucose increased NAD(P)H autofluorescence and the ATP/(ATP+ADP) ratio across the whole range of concentrations (Fig. 1i, j) and increased $[Ca^{2+}]_c$ and insulin secretion at 10 and 30 mmol/l (Fig. 1k, m; ESM Fig. 3), with a further increase on cell depolarisation with high K^+ . Glucose also increased the SP frequency recorded with multielectrode arrays (Fig. 1l; ESM Fig. 4), an effect that was inhibited by blocking all voltage-gated Ca^{2+} currents with Co^{2+} [24].

In G8-islets vs G5-islets, NAD(P)H was not significantly higher at 0.5 and 2 mmol/l glucose, the SP frequency was higher at all glucose concentrations, a rise in $[Ca^{2+}]_c$ and stimulation of insulin secretion was already detected at 5 mmol/l

glucose (Fig. 1i, k, l, m) and the maximal amplitude of insulin secretion was two to five times larger depending on the mode of expression (per islet, DNA content or insulin content) (ESM Fig. 3). Culture at G8 therefore slightly increased the sensitivity and markedly enhanced the maximal response to subsequent glucose stimulation.

In G20-islets, the initial NAD(P)H autofluorescence, SP frequency, $[Ca^{2+}]_c$ and insulin secretion after perfusion for 30 min at 0.5 mmol/l glucose were significantly higher vs G5-islets (Fig. 1i, k–o). The higher $[Ca^{2+}]_c$ and insulin secretion resulted from sustained closure of K_{ATP} channels with membrane depolarisation, as shown by their rapid reduction by the K_{ATP} channel opener diazoxide (Fig. 1n, o). Despite this persistent stimulation, NAD(P)H, the ATP/(ATP+ADP) ratio, $[Ca^{2+}]_c$ and insulin secretion further increased on stimulation with 5–10 mmol/l glucose. Above 10 mmol/l glucose, NAD(P)H and the ATP/(ATP+ADP) ratio plateaued, whereas SP frequency, $[Ca^{2+}]_c$ and insulin secretion abruptly decreased to a minimum [Fig. 1k, m, Δ (G30–G10)]. Thus, the acute $[Ca^{2+}]_c$ and insulin secretion glucose response curves in G20-islets looked 'bell-shaped' rather than 'sigmoid' as in G5-islets (Fig. 1k, m). In addition, the maximal rate of insulin secretion was larger in G20-islets than in G5-islets, irrespective of the mode of expression, but it was lower than in G8-islets when normalised to DNA content (ESM Fig. 3b), similar when normalised to islet number (ESM Fig. 3a) and much higher when normalised to insulin content (ESM Fig. 3c). Similar alterations in NAD(P)H, $[Ca^{2+}]_c$ and insulin secretion were observed after culture in FBS-free medium containing BSA (ESM Fig. 5).

We also measured the acute glucose-induced changes in $[Ca^{2+}]_c$ and insulin secretion during sustained depolarisation with 30 mmol/l extracellular K^+ in the presence of diazoxide (K30Dz). As shown in Fig. 1p, q, the addition of K30Dz to 0.5 mmol/l glucose stimulated insulin secretion to a larger extent in G8-islets and G20-islets than in G5-islets, despite similar increases in $[Ca^{2+}]_c$ levels. Subsequent stimulation with 10 mmol/l glucose reduced $[Ca^{2+}]_c$ to a larger extent in G5-islets whereas it decreased insulin secretion to a larger extent in G8-islets and G20-islets. There were, however, only transient changes in $[Ca^{2+}]_c$ and insulin secretion in all islet types on glucose changes from 10 to 30 mmol/l and then back to 10 mmol/l. These results suggest that the acute high glucose-induced reduction of $[Ca^{2+}]_c$ in G20-islets (Fig. 1k) resulted from acute plasma membrane repolarisation.

Characterisation of the acute $[Ca^{2+}]_c$ glucose response curve in human islets cultured under glucotoxic conditions As beta cells represent only \sim 50% of human islet cells, we used a RIP-driven D3cpv Ca^{2+} sensor to confirm that the glucotoxic alterations of islet $[Ca^{2+}]_c$ measured with fura2-LR occurred in

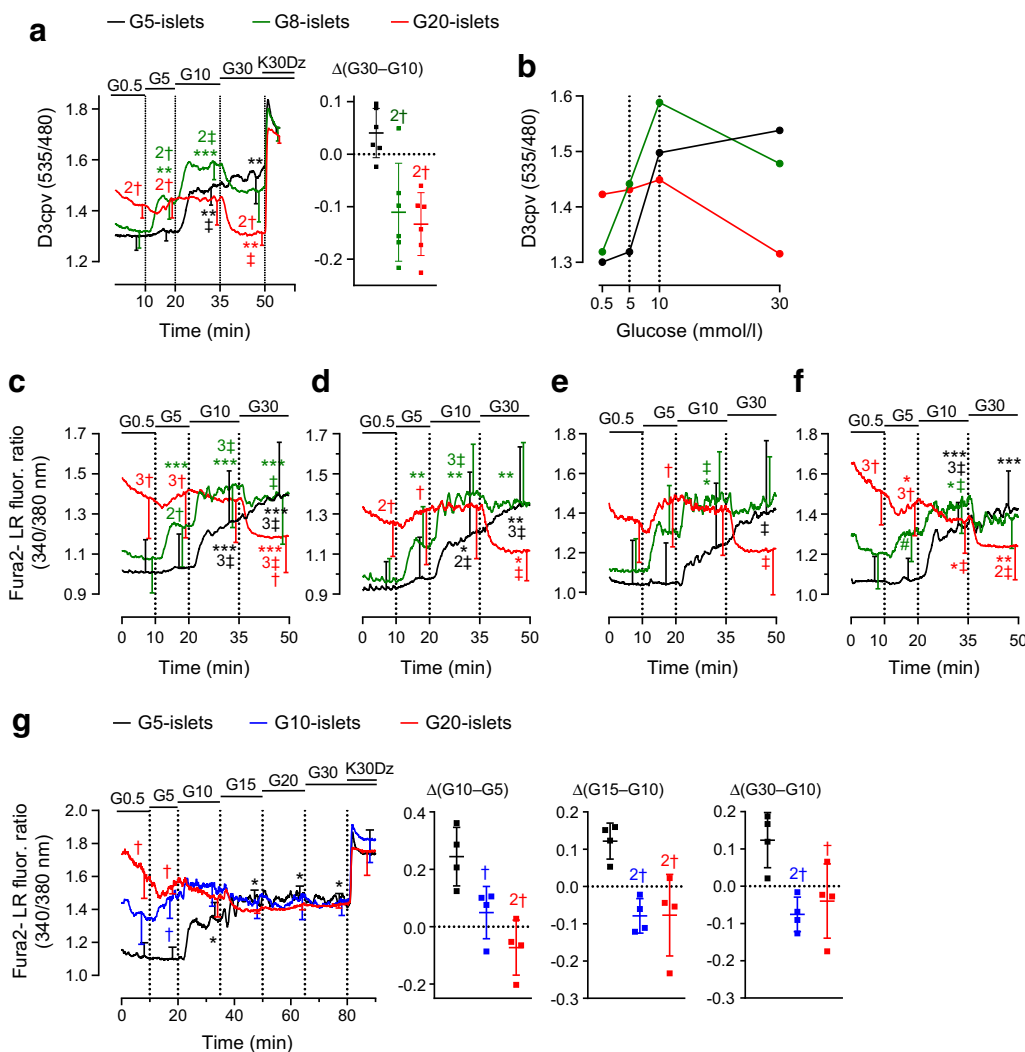
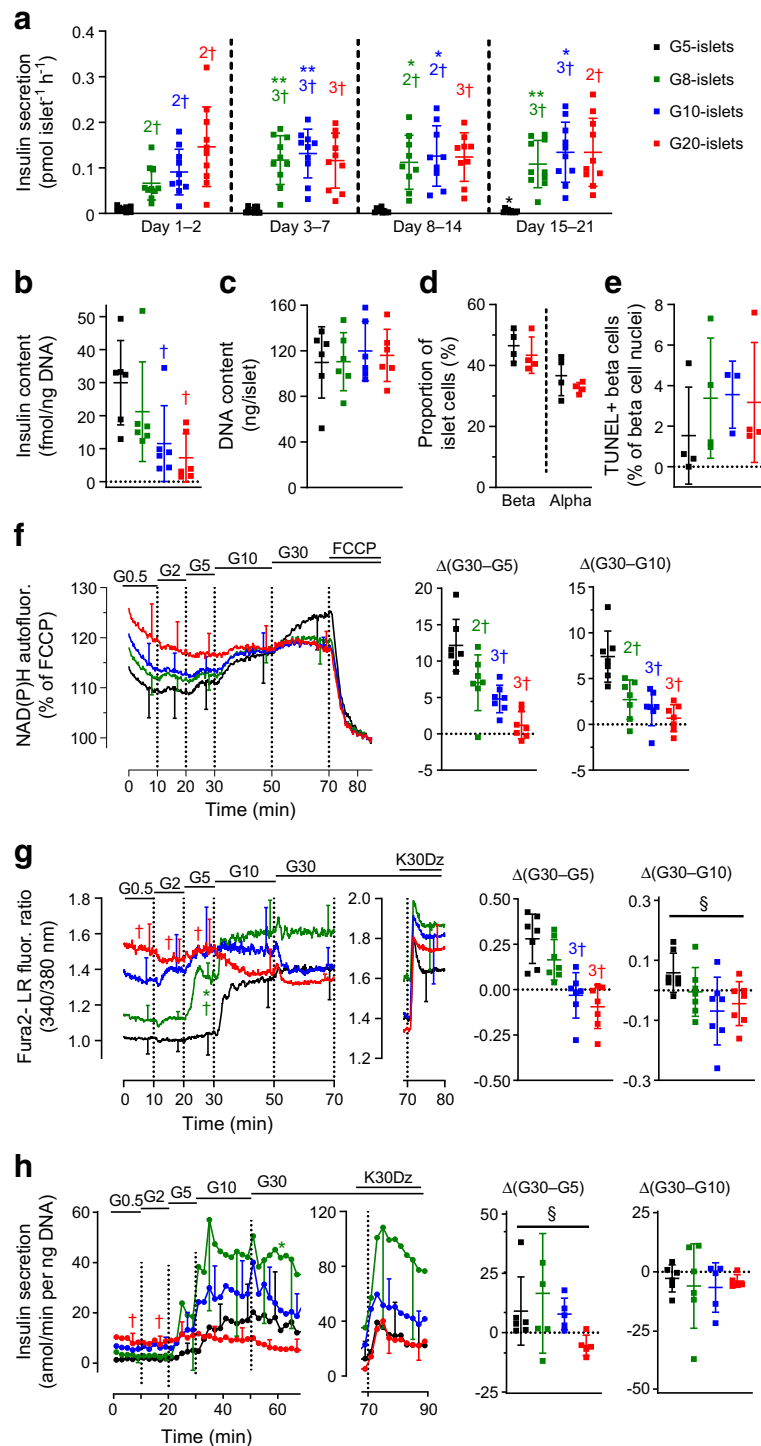


Fig. 2 Detailed analysis of the $[Ca^{2+}]_c$ glucose response curve in ND-islets. Islets were cultured as in Fig. 1 before measuring their acute functional responses to stepwise glucose stimulation (G5-islets, black; G8-islets, green; G10-islets, blue; G20-islets, red). **(a)** Changes in the beta cell D3cpv fluorescence ratio (Ad-RIP-D3cpv-infected islets) in response to glucose and K30Dz. The $\Delta(G30-G10)$ graph shows changes in the D3cpv fluorescence ratio between the indicated glucose steps, computed as for fura2-LR data in Fig. 1k. Means \pm SD for six islet preparations, each with two islets of each kind. **(b)** Acute $[Ca^{2+}]_c$ glucose response curves drawn from data in **(a)**. **(c-f)** Fura2-LR fluorescence ratio during stepwise glucose stimulation in 19 islet preparations that were different from the six preparations used in Fig. 1k **(c)** and in subgroups sorted according to the glucose step at which $[Ca^{2+}]_c$ was maximal in G20-islets **(d)**, maximal at 10 mmol/l glucose for seven preparations; **e**, maximal at 5

mmol/l glucose for five preparations; **f**, maximal at 0.5 mmol/l glucose for seven preparations). The mean $[Ca^{2+}]_c$ was computed over the 2 min preceding the last minute of each step. Data are means for the number of islet preparations. **(g)** Fura2-LR fluorescence ratio (as an indicator of $[Ca^{2+}]_c$) during stepwise glucose stimulation followed by membrane depolarisation with K30Dz. Means \pm SD for four preparations. The Δ graphs show the changes in fura2-LR fluorescence ratio between the indicated glucose steps calculated as in Fig. 1k using the mean ratio during the last 2 min of each step. Statistical analysis: Dynamic recordings, two-way ANOVA plus Tukey's test: * $p < 0.05$, ** $p < 0.01$ and *** $p < 0.001$ vs G0.5 step in the same islet type; † $p < 0.05$, 2† $p < 0.01$ and 3† $p < 0.001$ vs G5-islets at the same time point; ‡ $p < 0.05$, 2‡ $p < 0.01$ and 3‡ $p < 0.001$ vs previous step in the same islet type. Δ graphs, one-way ANOVA plus Dunnett's test: † $p < 0.05$ and 2† $p < 0.01$ vs G5-islets

beta cells (Fig. 2a; ESM Fig. 6). Interestingly, in these experiments, both G8-islets and G20-islets showed an acute inhibition of beta cell $[Ca^{2+}]_c$ above 10 mmol/l glucose. Thus, the acute $[Ca^{2+}]_c$ glucose response curves evolved from sigmoid in G5-islets to bell-shaped with a predominant increase in G8-islets to bell-shaped with a predominant inhibition in G20-islets (Fig. 2b).

We next measured islet $[Ca^{2+}]_c$ in 19 islet preparations that were different from the six preparations used in Fig. 1k to evaluate the variability in the glucotoxic alterations of $[Ca^{2+}]_c$ (Fig. 2c-f). The mean $[Ca^{2+}]_c$ traces were as in Fig. 1k, except that $[Ca^{2+}]_c$ was acutely inhibited above 10 mmol/l glucose not only in G20-islets but also in G8-islets (Fig. 2c). The alterations of $[Ca^{2+}]_c$



in G8-islets and G20-islets were not influenced by the isolation centre (ESM Fig. 7) or the donor sex, age and BMI (ESM Fig. 8). However, the glucose concentration at which $[Ca^{2+}]_c$ was maximal in G20-islets ranged from 10 to 0.5 mmol/l, generating slightly different types of acute $[Ca^{2+}]_c$ glucose response curves, with a drop in $[Ca^{2+}]_c$ above 10 mmol/l glucose as in Fig. 1k (Fig. 2d), from 5 to

10 mmol/l glucose (Fig. 2e) or from 5 to 30 mmol/l glucose (Fig. 2f).

We also determined the concentration of glucose required to acutely inhibit $[Ca^{2+}]_c$. In G20-islets, the inhibition was maximal on stimulation from 10 to 15 mmol/l glucose (Fig. 2g). In G10-islets, the $[Ca^{2+}]_c$ glucose response curve was also bell-shaped, with a maximum at 10 mmol/l glucose and an

Fig. 3 Very-long-term effects of glucose on cultured human islets. Islets were cultured for 3 weeks under the same conditions as in Fig. 1 (G5-islets, black; G8-islets, green; G10-islets, blue; G20-islets, red). **(a)** Insulin secreted in the culture medium, which was collected every 2–3 days; 7 day pooled data are shown for the last 2 weeks of culture. Means \pm SD and individual data for the ten preparations used for this figure. **(b)** Islet insulin/DNA content ratio and **(c)** DNA content after culture and perfusion shown in panel **(h)**. Means \pm SD and individual data for five to six preparations. **(d)** Proportions of beta and alpha cells and **(e)** percentage of TUNEL-positive beta cells in islet sections. Means \pm SD and individual data for three to four preparations. **(f)** NAD(P)H autofluorescence during stepwise glucose stimulation normalised to the fluorescence after 10 min in FCCP. Means \pm SD for seven preparations, each with one or two islets. **(g)** Fura2-LR fluorescence ratio and **(h)** insulin secretion rate during stepwise glucose stimulation followed by membrane depolarisation with K30Dz. Means \pm SD for seven **(g)** or five **(h)** preparations. The Δ graphs show the changes in **(f)** NAD(P)H autofluorescence, **(g)** fura2-LR fluorescence ratio and **(h)** insulin secretion rate between the indicated glucose steps, calculated as in Fig. 1. Statistical analysis: **(a)** Two-way ANOVA plus Tukey's test: * $p < 0.05$ and ** $p < 0.01$ vs day 1–2 in the same islet type; 2 $\dagger p < 0.01$ and 3 $\dagger p < 0.001$ vs G5-islets at the same time point. (**[b–e]** and Δ graphs in **[f–h]**) One-way ANOVA plus Dunnett's test: $\dagger p < 0.05$, 2 $\dagger p < 0.01$ and 3 $\dagger p < 0.001$ vs G5-islets; test for linear trend from left to right: $\S p < 0.05$

inhibition at 15 mmol/l glucose. Interestingly, the changes in $[Ca^{2+}]_c$ from 5 to 10 mmol/l glucose and from 10 to 15 mmol/l glucose were significantly lower in G10-islets and G20-islets than in G5-islets.

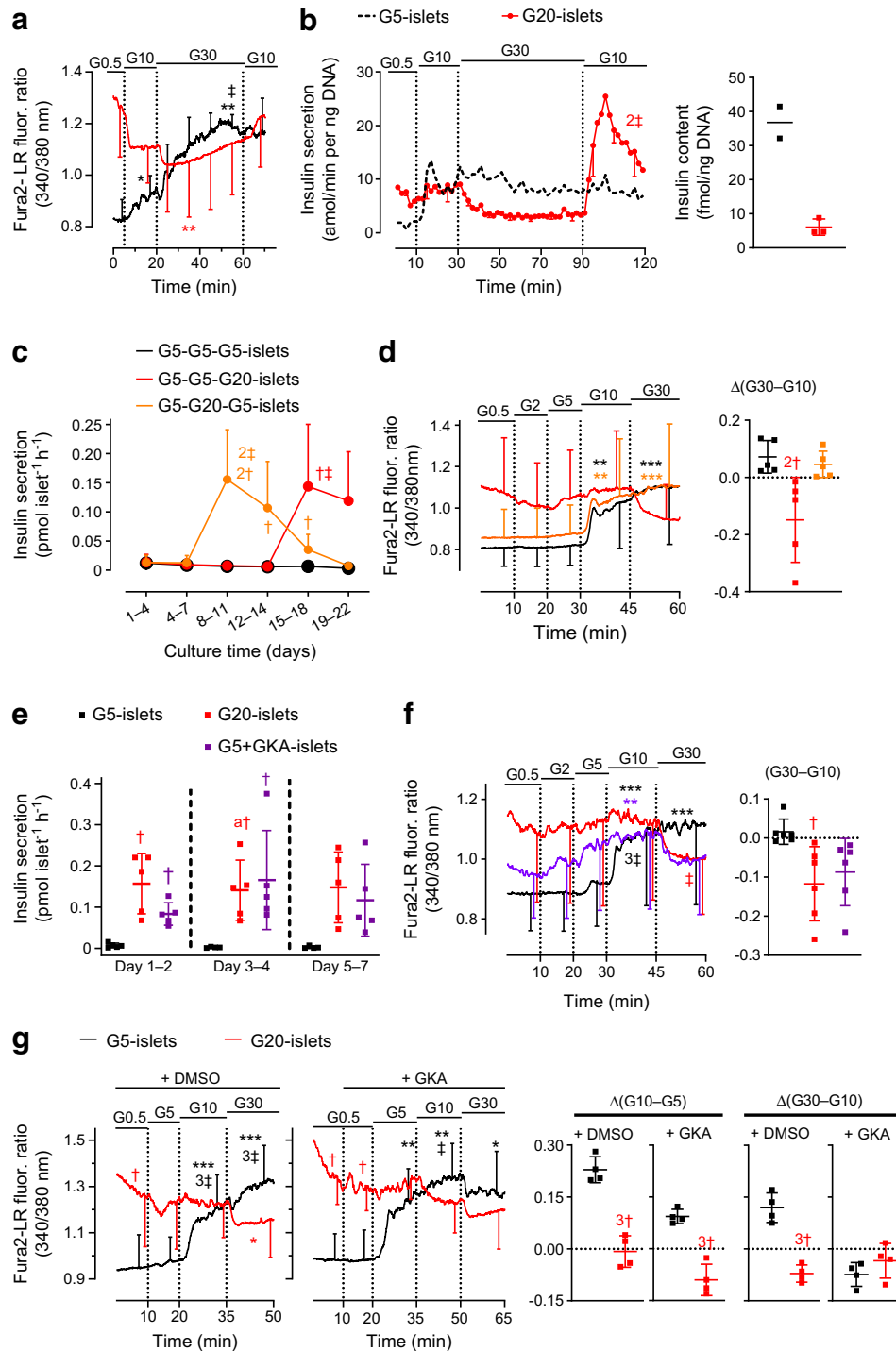
Impact of culture for 3 weeks at increasing glucose concentrations The islet characteristics and functional responses to acute stimulation with glucose were similar in islets cultured for 1 or 3 weeks at G5 (ESM Fig. 9). After 3 weeks at G8, G10 or G20 instead of G5, beta cell apoptosis did not increase significantly but insulin secretion during culture and other islet variables were affected as after 1 week of culture (Fig. 3; ESM Fig. 10). However, the alterations in GSIS and upstream coupling events were worse after 3 weeks of culture. After 3 weeks at G20, there was an almost complete lack of NAD(P)H response to glucose, an acute inhibition of $[Ca^{2+}]_c$ and insulin secretion on stimulation from 5 to 10–30 mmol/l glucose, and a lower maximal rate of insulin secretion than in G5-islets (except if expressed relative to insulin content) (Fig. 3f–h). After 3 weeks at G10, the acute glucose response curve for $[Ca^{2+}]_c$ and insulin secretion also looked bell-shaped rather than sigmoid (Fig. 3g, h).

Acute and chronic reversibility and role of glucose metabolism in the glucotoxic alterations in beta cell function The long-term culture of human islets at G10 or G20 revealed a bell-shaped acute glucose response curve for $[Ca^{2+}]_c$ and insulin secretion. In G20-islets, the drop in $[Ca^{2+}]_c$ and insulin secretion on stimulation from 10 to 30 mmol/l glucose lasted for at least 1 h and was acutely reversible on return to 10

mmol/l glucose, with a large rebound increase in insulin secretion (Fig. 4a, b). In addition, the long-term alterations of $[Ca^{2+}]_c$ responses in G20-islets were fully reversible after 1 week of culture at G5 (Fig. 4c, d), and the alteration after 1 week of culture at G20 was largely reproduced by pharmacological activation of glucokinase with Ro 28-0450 during culture at G5 (Fig. 4e, f). Finally, we tested the impact of acute glucokinase activation on the $[Ca^{2+}]_c$ responses of G5-islets and G20-islets (Fig. 4g). As expected, the glucose-induced changes in $[Ca^{2+}]_c$ were left-shifted by Ro 28-0450 in both G5-islets and G20-islets, with a significant acute inhibition of $[Ca^{2+}]_c$ in G20-islets above 5 mmol/l glucose + Ro 28-0450 rather than 10 mmol/l glucose alone.

Impact of culture for 1 week at increasing glucose concentrations on islets from donors with type 2 diabetes The glucotoxic alterations in beta cell function differ from the lower glucose sensitivity of insulin secretion usually described in patients with type 2 diabetes [25]. They also differ from the decrease in glucose sensitivity and maximal GSIS described in islets from type 2 diabetic donors and sometimes attributed to defective mitochondrial metabolism [15, 26–29]. However, these results were obtained in freshly isolated islets or after a short culture and did not show whether these functional alterations persisted after prolonged culture. We therefore tested the impact of 1 week of culture at G5, G8 or G20 on T2D-islets from six male donors (Table 1; ESM Table 1). As with ND-islets (Fig. 1a), insulin secretion by T2D-islets was higher during culture at G8 and G20 vs G5 (Fig. 5a). However, it was significantly lower than in six ND-islet preparations from ND donors of similar sex, age and BMI with similar cold ischaemia duration, islet purity and total culture duration (ESM Fig. 11). As in ND-islets, insulin content in T2D-islets was significantly lower after culture at G20 vs G5 (Fig. 5b; ESM Fig. 12a), whereas DNA content, percentage of TUNEL-positive beta cells and beta cell proportion were unaffected (Fig. 5c–e; ESM Fig. 12b, c). However, cytosolic E_{GSH} significantly increased after culture at G8 and G20 vs G5 (Fig. 5f; ESM Fig. 12d) while mitochondrial E_{GSH} was unaffected (Fig. 5g; ESM Fig. 12e), suggesting that, under glucotoxic conditions, T2D-islets experience higher cytosolic oxidative stress than ND-islets.

Regarding the metabolic responses to acute glucose, NAD(P)H recordings in T2D-islets cultured for 1 week at G5, G8 or G20 were similar to those of ND-islets cultured for 3 weeks at G20, with NAD(P)H levels that were already high in 0.5 mmol/l glucose and little glucose-induced rises in NAD(P)H despite the rapid decrease in FCCP (Fig. 5h; ESM Fig. 12f). Accordingly, data from two islet preparations from donors with type 2 diabetes suggested that the ATP/(ATP+ADP) ratio at low glucose was higher than in ND-islets and



only slightly increased at high glucose (ESM Fig. 13). Nevertheless, the $[Ca^{2+}]_c$ and insulin secretion responses to glucose after culture at G5 were qualitatively and quantitatively the same in T2D-islets and ND-islets (Fig. 5i, j; ESM Fig. 12g, h). Moreover, the alterations in T2D-islets after culture at G8 and G20 were qualitatively similar to those in ND-islets, except for two major differences in G8-islets: first, their

$[Ca^{2+}]_c$ and insulin secretion during perfusion at low glucose was slightly although not significantly higher than in G5-islets (Fig. 5i, ESM Fig. 12g, h); second, their insulin secretion significantly decreased on stimulation from 10 to 30 mmol/l glucose (Fig. 5i, j; ESM Fig. 12h, ESM Fig. 14). These results suggest that T2D-islets show functional signs of glucotoxicity at lower glucose concentration than ND-islets.

◀ **Fig. 4** Detailed analysis of the glucotoxic alterations in human beta cell function. **(a, b)** Acute reversibility. Islets were cultured for 1 week at G5 or G20 before measuring $[Ca^{2+}]_c$ and insulin secretion in response to various glucose concentrations, as shown at the top of the figure (G5-islets, black; G20-islets, red). The insulin/DNA content ratio was measured after perfusion. Data are means \pm SD for three to four preparations. The dashed trace shows the mean from two preparations as a reference but was not used for statistical analysis. **(c, d)** Long-term reversibility. Islets were cultured for a total of 3 weeks at the glucose concentrations shown for each consecutive week: G5-G5-G5 (3 weeks at G5; black), G5-G5-G20 (last week at G20; red), G5-G20-G5 (second week at G20 then 1 week at G5; orange). **(e)** Insulin secretion during culture with data pooled over 3- to 4-day periods. Means \pm SD for nine preparations. **(d)** $[Ca^{2+}]_c$ responses to stepwise glucose stimulation and K30Dz. Means \pm SD for five preparations. The Δ graph shows the difference in fura2-LR fluorescence ratios between 10 and 30 mmol/l glucose. **(e, f)** Impact of pharmacological glucokinase activation during culture. Islets were cultured for 1 week in G5 + DMSO 1/1000 (G5-islets, black), G20 + DMSO 1/1000 (G20-islets, red) or G5 + 3 μ mol/l Ro 28-0450, a glucokinase activator (G5+GKA-islets, purple). **(e)** Insulin secretion in the medium collected at the end of day 2, day 4 and day 7 of culture. Means \pm SD and individual data for five preparations. **(f)** $[Ca^{2+}]_c$ responses to stepwise glucose stimulation and K30Dz. Means \pm SD for six preparations. The Δ (G30–G10) graph shows the difference in fura2-LR fluorescence ratios between 10 and 30 mmol/l glucose. **(g)** Impact of acute pharmacological glucokinase activation. Islets were cultured for 1 week in RPMI medium containing G5 or G20 (G5-islets, black; G20-islets, red). The graphs show $[Ca^{2+}]_c$ responses to acute glucose stimulation in the presence of DMSO 1/1000 (+DMSO) or 3 μ mol/l GKA (+GKA) as shown at the top of the graphs. The Δ graphs show the differences in fura2-LR fluorescence ratios between the indicated glucose concentrations in the presence of DMSO or GKA. Means \pm SD for four preparations. Statistical analysis: **(a, c, e)** and dynamic recordings in **(b, d, f, g)** Two-way ANOVA plus Tukey's test: * p <0.05, ** p <0.01 and *** p <0.001 vs G0.5 step in the same islet type; † p <0.05 and 2† p <0.01 vs G5-islets at the same time point; ‡ p <0.05, 2‡ p <0.01 and 3‡ p <0.001 vs previous step in the same islet type. (Δ graphs in **(b, d, f, g)**) One-way ANOVA plus Dunnett's test: † p <0.05, 2† p <0.01 and 3† p <0.001 vs G5-islets

Discussion

Human islets cultured for up to 3 weeks under glucotoxic conditions (G8, G10 and G20 vs G5) displayed strong alterations in GSIS and upstream coupling events but no significant increase in beta cell apoptosis (for further details see ESM Discussion) or oxidative stress. Among the glucotoxic alterations in human beta cell function, the lower insulin content, the left-shifted glucose response curve with higher mitochondrial metabolism and rate of secretion at low glucose, and the lower amplitude of the maximal glucose response have been reported previously [15, 30–35]. However, the alterations in acute $[Ca^{2+}]_c$ and insulin secretion glucose response curves from sigmoid to bell-shaped, with maximal stimulation at 5 or 10 mmol/l glucose and paradoxical inhibition above that concentration, have not been reported previously. These alterations occurred in beta cells and were almost systematically observed, irrespective of the available donor characteristics, including a history of type 2 diabetes.

Possible mechanism The acute glucose-induced inhibition of $[Ca^{2+}]_c$ and insulin secretion in glucotoxic islets is unlikely to have resulted from an increase in beta cell apoptosis, as shown by their normalisation after another week of culture at G5 and by the lack of a significant increase in beta cell apoptosis. This inhibition is likely to have resulted from an acute repolarisation of the plasma membrane owing to changes in ion channel activity, as it was not observed in K30-depolarised islets. It did not, however, result from an acute inhibition of glucose metabolism. Indeed, although the glucotoxic alteration of GSIS in human islets is usually considered to result from defective mitochondrial metabolism [28, 36], measuring NAD(P)H and the ATP/(ATP+ADP) ratio normalised to FCCP or azide unequivocally confirmed that, in human as in rat islets cultured under glucotoxic conditions, mitochondrial metabolism was markedly increased at low glucose concentrations rather than decreased at high glucose concentrations [21, 34]. In our study, such an increase at low glucose concentrations was also observed in T2D-islets cultured at G5 for ~10 days and was further augmented by culture at G20, in contrast to studies showing that mitochondrial metabolism is markedly reduced in T2D-islets [12, 15, 36–38]. The glucotoxic alterations of human beta cell function that we observed may therefore result from overstimulation of glucose metabolism (perhaps resulting from increased glucokinase activity [39]) with the eventual activation of a repolarising current on a further rise in glucose concentration. It remains possible, however, that other changes in metabolic coupling factors, for example divergent changes in NADH, NADPH and adenine nucleotides between the cytosol and mitochondrial matrix, underlie the acute glucose-induced inhibition of $[Ca^{2+}]_c$ and insulin secretion. Alterations in cAMP signalling and distal Ca^{2+} exocytosis coupling events may also reduce GSIS independently from alterations in $[Ca^{2+}]_c$ responses [40, 41].

Pathophysiological relevance The acute glucose-induced inhibition of $[Ca^{2+}]_c$ and insulin secretion was mainly studied in G20-islets stimulated above 10 mmol/l glucose, questioning its pathophysiological relevance. However, we have evidence that this inhibition occurs at lower glucose concentrations that can be encountered in patients with type 2 diabetes undergoing an OGTT [25]. First, in ~50% of the preparations, the drop in $[Ca^{2+}]_c$ in G20-islets was already detected on stimulation from 5 to 10 mmol/l glucose. Second, the drop in $[Ca^{2+}]_c$ was observed in G10-islets, in most beta cell-specific $[Ca^{2+}]_c$ recordings in G8-islets, and in T2D-islets cultured at G8. The alterations in GSIS and upstream coupling events in ND-islets cultured at G8 and G10 merit further discussion. The left shift of their glucose response curves and marked increase in maximal GSIS could be a beneficial adaptation to a moderate increase in glucose concentration. However,

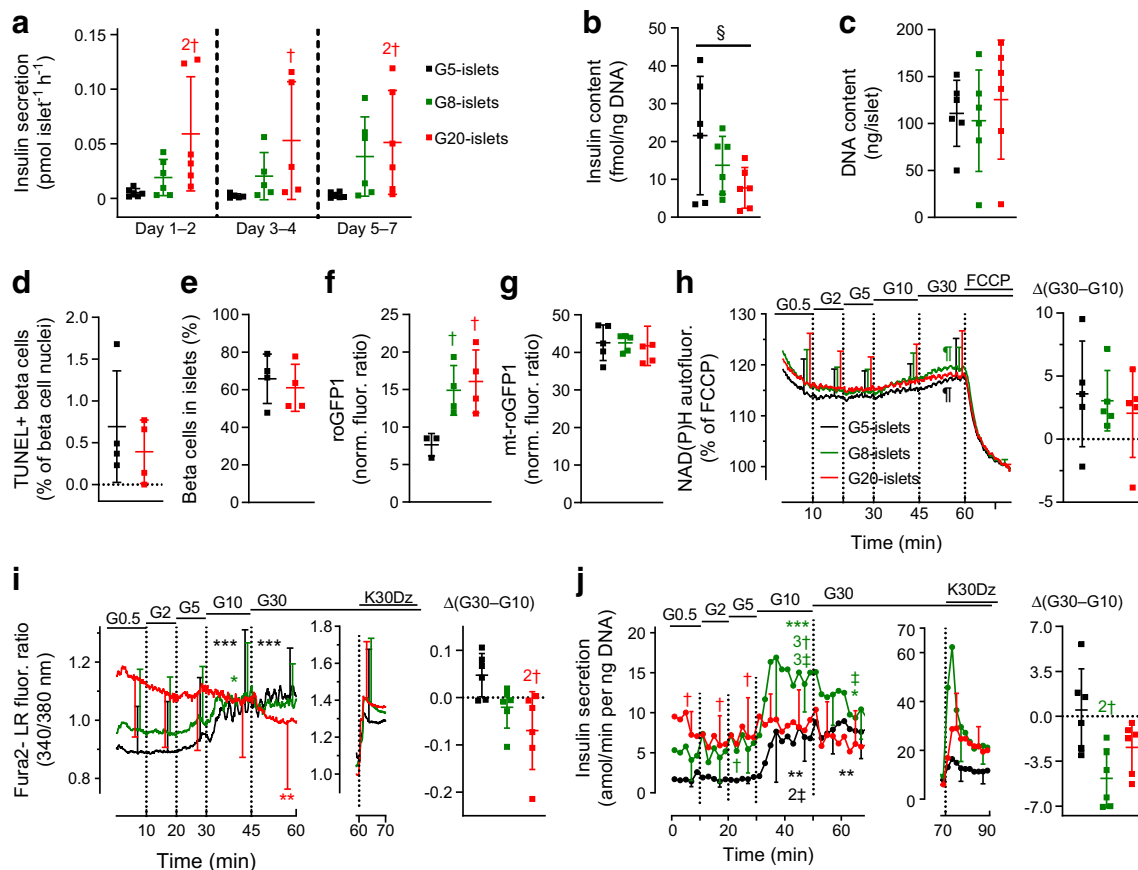


Fig. 5 Long-term effects of glucose on cultured islets from type 2 diabetic donors. After preculture, islets from donors with type 2 diabetes were cultured for 1 week in RPMI medium containing G5, G8 or G20 (G5-islets, black; G8-islets, green; G20-islets, red). **(a)** Insulin secreted in the culture medium collected every 2–3 days. Means \pm SD and individual data for five to six preparations. **(b)** Islet insulin and **(c)** DNA content after perfusion shown in panel **(i)**. Means \pm SD and individual data for six preparations. **(d, e)** Percentages of apoptotic beta cells **(d)** and proportions of beta cells **(e)** measured in the same islet sections. Means \pm SD and individual data for four preparations. **(f)** Cytosolic and **(g)** mitochondrial glutathione oxidation measured as in Fig. 1g,h. Means \pm SD and individual data for three to four **(f)** and five **(g)** preparations. **(h)** NAD(P)H autofluorescence during stepwise glucose stimulation normalised to the fluorescence after 10 min in FCCP. Means \pm SD for five preparations. **(i)**

Fura2-LR fluorescence ratio and **(j)** insulin secretion rate during stepwise glucose stimulation followed by membrane depolarisation with K30Dz. The islet insulin/DNA content ratio was measured after perfusion. Means \pm SD for six preparations. The Δ graphs show changes in **(h)** NAD(P)H autofluorescence, **(i)** fura2-LR fluorescence ratio and **(j)** insulin secretion rate between the indicated glucose steps. Statistical analysis: ([a] and dynamic recordings in [h–j]) Two-way ANOVA plus Tukey’s test: * p <0.05, ** p <0.01 and *** p <0.001 vs G0.5 step in the same islet type; † p <0.05, ‡ p <0.01 and ‡ p <0.001 vs G5-islets at the same time point; ‡ p <0.05, ‡ p <0.01 and ‡ p <0.001 vs previous step in the same islet type; ‡ p <0.05 vs G2 step in the same islet type. ([b–g] and Δ graphs in [h–j]) One-way ANOVA plus Dunnett’s test: † p <0.05 and ‡ p <0.01 vs G5-islets; test for linear trend from left to right § p <0.05

the bell-shaped curves with acute inhibition of $[Ca^{2+}]_c$ above 10 mmol/l glucose and the larger variability of their insulin secretion response to acute stimulation from 10 to 30 mmol/l glucose suggest that these islets are close to the tipping point between beta cell adaptation and decompensation. The corresponding blood glucose level at which such a process would occur in vivo is, however, difficult to estimate.

How do our results change our understanding of beta cell pathophysiology in type 2 diabetes? The role of glucotoxicity in the development of glucose intolerance and type 2 diabetes remains questionable; however, its role in established type 2

diabetes is clearer [13, 42]. As (gluco)lipotoxic culture conditions trigger apoptosis and irreversible defects in GSIS [15], and because fast recovery of the beta cell mass is unlikely, the rapid improvement of GSIS and remission of type 2 diabetes in recently diagnosed patients submitted to a diet very low in energy [16, 17] is likely to have resulted from correction of glucotoxic beta cell dysfunction. If the acute glucose-induced inhibition of insulin secretion we observed above 5–10 mmol/l glucose in glucotoxic human islets is operational in patients with type 2 diabetes, it may contribute to the lack of an appropriate increase or even to a decrease in insulin secretion after meals. Interestingly, it was previously reported that, in murine models of diabetes with mouse and human islets

transplanted under the kidney capsule, glucose injection acutely decreased human plasma insulin while increasing mouse insulin, suggesting that this glucotoxic phenotype is operational *in vivo* [14]. The observation of a bell-shaped insulin secretion glucose response curve during pancreas perfusion in Zucker diabetic fatty rats [43] reinforces the hypothesis that this glucotoxic alteration is operational in diabetic islets *in vivo*. In that scenario, a reduction in beta cell glucose metabolism could restore a sigmoid acute glucose response curve (for $[Ca^{2+}]_c$ and insulin secretion) and restore a rise in insulin secretion after meals. In support of this hypothesis, it has been shown that inhibition of glucokinase or the mitochondrial pyruvate transporter in models of beta cell glucotoxicity or diabetes reduced beta cell stimulation at low glucose concentrations, right-shifted the $[Ca^{2+}]_c$ and insulin secretion glucose response curves and thereby improved $[Ca^{2+}]_c$ oscillations and GSIS [34, 44, 45]. Thus, identifying the molecular mechanism of the acute glucose-induced inhibition of $[Ca^{2+}]_c$ and insulin secretion beyond acute membrane repolarisation may help to identify new putative therapeutic targets to improve beta cell function in recent-onset type 2 diabetes.

Considerations about donors, islet shipment, culture conditions and islet characteristics This study was carried out with islets from donors from five different sources covering a large range of ages and BMI with or without a history of type 2 diabetes. The islet preparations were selected based on their high islet purity and the possibility of shipping islets in a maximum of 3 days. The size of the islets without central necrosis detected at $\times 10$ magnification was rather large, limiting the validity of the study to islets with a diameter between 75 and 330 μm . However, except for the high male/female sex ratio and high prevalence of obesity (Table 1), the clinical characteristics of the donors were unremarkable. Although we used different sets of preparations for each type of measurement, the alterations in the $[Ca^{2+}]_c$ responses to glucose were largely similar across the 27 islet preparations tested.

The time between isolation and reception in the laboratory varied considerably between islet sources. Because we cultured islets for at least 10 days, we consider that this variable should not have affected our results. Moreover, the long preculture and culture time can be considered as a strength of our study, as it allowed us to assess beta cell function at a distance from the events preceding donor death and to study the intrinsic alteration of beta cell function that persists in islets from donors with type 2 diabetes after 10–15 days of culture at G5.

Finally, isolated islets are no longer vascularised and innervated, which may alter their response to glucose, thereby limiting the pathophysiological relevance of *in vitro* studies.

In this context, the islet size is important, as diffusion of oxygen/nutrients to the centre decreases with increase in diameter. From their DNA content, we estimated that islets with a diameter of $\sim 250 \mu\text{m}$ contained $\sim 12,000$ cells (of which ~ 6000 are beta cells). Although we cannot exclude that limited access to nutrients/oxygen contributed to the glucotoxic phenotype, the alterations in the $[Ca^{2+}]_c$ responses occurred at the islet periphery where *fura2-LR*-acetoxymethylester loading and adenoviral infection are optimal.

Conclusion Prolonged culture of human islets from non-diabetic or type 2 diabetic donors under moderate to severe glucotoxic conditions markedly increased their glucose sensitivity and changed their acute glucose response curve for changes in $[Ca^{2+}]_c$ and insulin secretion from sigmoid to bell-shaped, with maximal stimulation at 5 or 10 mmol/l glucose and paradoxical inhibition above that concentration. If the latter glucose-induced inhibition is operational *in vivo*, characterising its underlying mechanism may help identify new ways to improve beta cell function and reverse recently diagnosed type 2 diabetes.

Supplementary Information The online version of this article (<https://doi.org/10.1007/s00125-022-05842-y>) contains peer-reviewed but unedited supplementary material.

Acknowledgements We thank F. B. Aissa, N. Antoine and F. Knockaert (Université catholique de Louvain) for expert technical help. We also thank J.-C. Henquin (Université catholique de Louvain) for critical reading of the paper and J. Lang (University of Bordeaux) for helpful discussion. We thank F. Vachier-Lahaye from the Coordination des dons d'organes and the Centre de Ressources Biologiques (CRB; Identifiant BIOBANQUES – BB-0033-00031) from CHU Montpellier for the human islet preparations.

Data availability All data generated or analysed during this study are included in this published article and its electronic supplementary material. For further information, please write to the corresponding author.

Funding This study was funded by the Bridge project DiaType from the Brussels Capital Region – Innoviris; Action de Recherche Concertée 18/23-094 from the Communauté française de Belgique; grant SFD 2019 from the Société Francophone du Diabète (Paris, France); grant 1912-03555 from the Leona M. and Harry B. Helmsley Charitable Trust; and the Fonds de la Recherche Scientifique-FNRS equipment grants U.N023.18 and U.N033.21, CDR research grant J.0087.19 and PDR research grants T.0124.15 and T.0110.20. J-CJ and PG are Research Directors of the Fonds de la Recherche Scientifique-FNRS, Brussels, Belgium. AHdS is the recipient of an FSR ‘incoming postdoctoral fellowship’ from UCLouvain. MR and MJ were supported by a Ministère de l'Éducation Nationale, de l'Enseignement Supérieur et de la Recherche ‘Excellence PhD Scholarship’ and by grant DIABLO ANR-18-CE17-0005, France. Some human islet preparations were provided through JDRF award 31-2008-416 (ECIT Islet for Basic Research program) and the NIDDK-funded Integrated Islet Distribution Program (IIDP) (RRID:SCR_014387) at the Southern California Islet Cell Resource Center, City of Hope, USA (NIH Grant #2UC4DK098085). The study funders were not involved in the design of the study, the collection, analysis and interpretation of data or writing of the report and did not impose any restrictions regarding the publication of the report.

Authors' relationships and activities J-CJ is a member of the *Diabetologia* Editorial Board. The other authors declare that there are no relationships or activities that might bias, or be perceived to bias, their work.

Contribution statement J-CJ, AW, CB, MR and PG conceived and designed the experiments. AW and CB set up the human islet isolation procedures in Montpellier. AB and NIM isolated human islets in Brussels. MT, AHdS, HC, MJ, MB, A-FC, J-PD and LRBS performed the experiments. MT, MR and J-CJ analysed the data. MT and J-CJ wrote the paper and all authors edited and approved the paper. J-CJ is the guarantor of this work and, as such, had full access to all the data in the study and takes responsibility for the integrity of the data and the accuracy of the data analysis.

References

- Henquin JC, Dufrane D, Nenquin M (2006) Nutrient control of insulin secretion in isolated normal human islets. *Diabetes* 55(12):3470–3477. <https://doi.org/10.2337/db06-0868>
- Henquin JC, Dufrane D, Kerr-Conte J, Nenquin M (2015) Dynamics of glucose-induced insulin secretion in normal human islets. *Am J Physiol Endocrinol Metab* 309(7):E640–E650. <https://doi.org/10.1152/ajpendo.00251.2015>
- Rorsman P, Ashcroft FM (2018) Pancreatic β -cell electrical activity and insulin secretion: Of mice and men. *Physiol Rev* 98(1):117–214. <https://doi.org/10.1152/physrev.00008.2017>
- Henquin JC (2009) Regulation of insulin secretion: a matter of phase control and amplitude modulation. *Diabetologia* 52(5):739–751. <https://doi.org/10.1007/s00125-009-1314-y>
- Rahier J, Guiot Y, Goebbels RM, Sempoux C, Henquin JC (2008) Pancreatic β -cell mass in European subjects with type 2 diabetes. *Diabetes Obes Metab* 10(Suppl 4):32–42. <https://doi.org/10.1111/j.1463-1326.2008.00969.x>
- Turner RC, Cull CA, Frighi V, Holman RR (1999) Glycemic control with diet, sulfonylurea, metformin, or insulin in patients with type 2 diabetes mellitus: progressive requirement for multiple therapies (UKPDS 49). UK Prospective Diabetes Study (UKPDS) Group. *JAMA* 281(21):2005–2012. <https://doi.org/10.1001/jama.281.21.2005>
- Andersson A, Hellerstrom C (1972) Metabolic characteristics of isolated pancreatic islets in tissue culture. *Diabetes* 21(2 Suppl):546–554. <https://doi.org/10.2337/diab.21.2.s546>
- Poitout V, Robertson RP (2008) Glucolipotoxicity: fuel excess and β -cell dysfunction. *Endocr Rev* 29(3):351–366. <https://doi.org/10.1210/er.2007-0023>
- van Raalte DH, Diamant M (2011) Glucolipotoxicity and beta cells in type 2 diabetes mellitus: target for durable therapy? *Diabetes Res Clin Pract* 93(Suppl 1):S37–S46. [https://doi.org/10.1016/S0168-8227\(11\)70012-2](https://doi.org/10.1016/S0168-8227(11)70012-2)
- Bensellam M, Laybutt DR, Jonas JC (2012) The molecular mechanisms of pancreatic beta-cell glucotoxicity: Recent findings and future research directions. *Mol Cell Endocrinol* 364(1–2):1–27. <https://doi.org/10.1016/j.mce.2012.08.003>
- Prentki M, Peyot ML, Masiello P, Murthy Madiraju SR (2020) Nutrient-induced metabolic stress, adaptation, detoxification, and toxicity in the pancreatic β -cell. *Diabetes* 69(3):279–290. <https://doi.org/10.2337/dbi19-0014>
- Lytrivi M, Castell AL, Poitout V, Cnop M (2020) Recent insights into mechanisms of β -cell lipo- and glucolipotoxicity in type 2 diabetes. *J Mol Biol* 432(5):1514–1534. <https://doi.org/10.1016/j.jmb.2019.09.016>
- Weir GC (2020) Glucolipotoxicity, beta-cells, and diabetes: the emperor has no clothes. *Diabetes* 69(3):273–278. <https://doi.org/10.2337/db19-0138>
- Dai C, Kayton NS, Shostak A et al (2016) Stress-impaired transcription factor expression and insulin secretion in transplanted human islets. *J Clin Invest* 126(5):1857–1870. <https://doi.org/10.1172/JCI83657>
- Marselli L, Piron A, Suleiman M et al (2020) Persistent or transient human β cell dysfunction induced by metabolic stress: specific signatures and shared gene expression with type 2 diabetes. *Cell Rep* 33(9):108466–108466. <https://doi.org/10.1016/j.celrep.2020.108466>
- Lim EL, Hollingsworth KG, Aribisala BS, Chen MJ, Mathers JC, Taylor R (2011) Reversal of type 2 diabetes: normalisation of beta cell function in association with decreased pancreas and liver triacylglycerol. *Diabetologia* 54(10):2506–2514. <https://doi.org/10.1007/s00125-011-2204-7>
- Taylor R, Al-Mrabeh A, Zhyzhneuskaya S et al (2018) Remission of human type 2 diabetes requires decrease in liver and pancreas fat content but is dependent upon capacity for beta cell recovery. *Cell Metab* 28(4):547–556; e541–e543. <https://doi.org/10.1016/j.cmet.2018.07.003>
- de Souza AH, Santos LRB, Roma LP, Bensellam M, Carpinelli AR, Jonas JC (2017) NADPH oxidase-2 does not contribute to beta-cell glucotoxicity in cultured pancreatic islets from C57BL/6J mice. *Mol Cell Endocrinol* 439:354–362. <https://doi.org/10.1016/j.mce.2016.09.022>
- Roma LP, Jonas JC (2020) Nutrient metabolism, subcellular redox state, and oxidative stress in pancreatic islets and beta-cells. *J Mol Biol* 432(5):1461–1493. <https://doi.org/10.1016/j.jmb.2019.10.012>
- Detimary P, Jonas JC, Henquin JC (1996) Stable and diffusible pools of nucleotides in pancreatic islet cells. *Endocrinology* 137(11):4671–4676. <https://doi.org/10.1210/endo.137.11.8895332>
- Khalidi MZ, Guiot Y, Gilon P, Henquin JC, Jonas JC (2004) Increased glucose sensitivity of both triggering and amplifying pathways of insulin secretion in rat islets cultured for 1 wk in high glucose. *Am J Physiol Endocrinol Metab* 287(2):E207–E217. <https://doi.org/10.1152/ajpendo.00426.2003>
- Jaffredo M, Bertin E, Pirog A et al (2021) Dynamic uni- and multicellular patterns encode biphasic activity in pancreatic islets. *Diabetes* 70(4):878–888. <https://doi.org/10.2337/db20-0214>
- Lebreton F, Pirog A, Belouah I et al (2015) Slow potentials encode intercellular coupling and insulin demand in pancreatic beta cells. *Diabetologia* 58(6):1291–1299. <https://doi.org/10.1007/s00125-015-3558-z>
- Braun M, Ramracheya R, Bengtsson M et al (2008) Voltage-gated ion channels in human pancreatic beta-cells: electrophysiological characterization and role in insulin secretion. *Diabetes* 57(6):1618–1628. <https://doi.org/10.2337/db07-0991>
- Ferrannini E, Mari A (2014) beta-Cell function in type 2 diabetes. *Metabolism* 63(10):1217–1227. <https://doi.org/10.1016/j.metabol.2014.05.012>
- Doliba NM, Qin W, Najafi H et al (2012) Glucokinase activation repairs defective bioenergetics of islets of Langerhans isolated from type 2 diabetics. *Am J Physiol Endocrinol Metab* 302(1):E87–E102. <https://doi.org/10.1152/ajpendo.00218.2011>
- Li G, Wu B, Ward MG et al (2016) Multifunctional in vivo imaging of pancreatic islets during diabetes development. *J Cell Sci* 129(14):2865–2875. <https://doi.org/10.1242/jcs.190843>
- Brereton MF, Rohm M, Shimomura K et al (2016) Hyperglycaemia induces metabolic dysfunction and glycogen accumulation in pancreatic beta-cells. *Nat Commun* 7:13496. <https://doi.org/10.1038/ncomms13496>
- Nagao M, Esguerra JLS, Asai A et al (2020) Potential protection against type 2 diabetes in obesity through lower CD36 expression

- and improved exocytosis in beta-cells. *Diabetes* 69(6):1193–1205. <https://doi.org/10.2337/db19-0944>
30. Ling Z, Pipeleers DG (1996) Prolonged exposure of human β cells to elevated glucose levels results in sustained cellular activation leading to a loss of glucose regulation. *J Clin Invest* 98(12):2805–2812. <https://doi.org/10.1172/JCI119108>
 31. Eizirik DL, Korbutt GS, Hellerström C (1992) Prolonged exposure of human pancreatic islets to high glucose concentrations in vitro impairs the β -cell function. *J Clin Invest* 90(4):1263–1268. <https://doi.org/10.1172/JCI115989>
 32. Bjorklund A, Lansner A, Grill VE (2000) Glucose-induced $[Ca^{2+}]_i$ abnormalities in human pancreatic islets: important role of overstimulation. *Diabetes* 49(11):1840–1848. <https://doi.org/10.2337/diabetes.49.11.1840>
 33. Masini M, Anello M, Bugliani M et al (2014) Prevention by metformin of alterations induced by chronic exposure to high glucose in human islet beta cells is associated with preserved ATP/ADP ratio. *Diabetes Res Clin Pract* 104(1):163–170. <https://doi.org/10.1016/j.diabres.2013.12.031>
 34. Chareyron I, Christen S, Moco S et al (2020) Augmented mitochondrial energy metabolism is an early response to chronic glucose stress in human pancreatic beta cells. *Diabetologia* 63(12):2628–2640. <https://doi.org/10.1007/s00125-020-05275-5>
 35. Mir-Coll J, Moede T, Paschen M et al (2021) Human islet microtissues as an in vitro and an in vivo model system for diabetes. *Int J Mol Sci* 22(4):1813. <https://doi.org/10.3390/ijms22041813>
 36. Ma Z, Wirstrom T, Borg LAH et al (2012) Diabetes reduces β -cell mitochondria and induces distinct morphological abnormalities, which are reproducible by high glucose in vitro with attendant dysfunction. *Islets* 4(3):233–242. <https://doi.org/10.4161/isl.20516>
 37. Anello M, Lupi R, Spampinato D et al (2005) Functional and morphological alterations of mitochondria in pancreatic beta cells from type 2 diabetic patients. *Diabetologia* 48(2):282–289. <https://doi.org/10.1007/s00125-004-1627-9>
 38. Haythorne E, Rohm M, van de Bunt M et al (2019) Diabetes causes marked inhibition of mitochondrial metabolism in pancreatic β -cells. *Nat Commun* 10(1):2474–2474. <https://doi.org/10.1038/s41467-019-10189-x>
 39. Chen C, Hosokawa H, Bumbalo LM, Leahy JL (1994) Regulatory effects of glucose on the catalytic activity and cellular content of glucokinase in the pancreatic beta cell. Study using cultured rat islets. *J Clin Invest* 94(4):1616–1620. <https://doi.org/10.1172/JCI117503>
 40. Roger B, Papin J, Vacher P et al (2011) Adenylyl cyclase 8 is central to glucagon-like peptide 1 signalling and effects of chronically elevated glucose in rat and human pancreatic beta cells. *Diabetologia* 54(2):390–402. <https://doi.org/10.1007/s00125-010-1955-x>
 41. Dubois M, Vacher P, Roger B et al (2007) Glucotoxicity inhibits late steps of insulin exocytosis. *Endocrinology* 148(4):1605–1614. <https://doi.org/10.1210/en.2006-1022>
 42. Weir GC, Butler PC, Bonner-Weir S (2021) The beta-cell glucose toxicity hypothesis: Attractive but difficult to prove. *Metabolism* 124:154870. <https://doi.org/10.1016/j.metabol.2021.154870>
 43. Zhou YP, Cockburn BN, Pugh W, Polonsky KS (1999) Basal insulin hypersecretion in insulin-resistant Zucker diabetic and Zucker fatty rats: role of enhanced fuel metabolism. *Metabolism* 48(7):857–864. [https://doi.org/10.1016/S0026-0495\(99\)90219-6](https://doi.org/10.1016/S0026-0495(99)90219-6)
 44. Jahan I, Corbin KL, Bogart AM et al (2019) Reducing glucokinase activity restores endogenous pulsatility and enhances insulin secretion in islets from db/db mice. *Endocrinology* 159:3747–3760. <https://doi.org/10.1210/en.2018-00589>
 45. Nakamura A, Omori K, Terauchi Y (2021) Glucokinase activation or inactivation: which will lead to the treatment of type 2 diabetes? *Diabetes Obes Metab* 23(10):2199–2206. <https://doi.org/10.1111/dom.14459>

Publisher's note Springer Nature remains neutral with regard to jurisdictional claims in published maps and institutional affiliations.

Springer Nature or its licensor (e.g. a society or other partner) holds exclusive rights to this article under a publishing agreement with the author(s) or other rightsholder(s); author self-archiving of the accepted manuscript version of this article is solely governed by the terms of such publishing agreement and applicable law.